

Projecting the compound effects of climate change and white-nose syndrome on North American bat species

Meredith McClure¹, Sarah Olson¹, Catherine Haase¹, Liam McGuire¹, C. Hranac¹, Cori Lausen¹, Raina Plowright¹, Nathan Fuller¹, and David Hayman¹

¹Affiliation not available

May 26, 2021

Abstract

Climate change and disease are threats to biodiversity that may compound and interact with one another in ways that are difficult to predict. White-nose syndrome (WNS), caused by a cold-loving fungus (*Pseudogymnoascus destructans*), has had devastating impacts on North American hibernating bats, and impact severity has been linked to hibernaculum microclimate conditions. As WNS spreads across the continent and climate conditions change, anticipating these stressors' combined impacts may improve conservation outcomes for bats. We build on the recent development of winter species distribution models for five North American bat species, which used a hybrid correlative-mechanistic approach to integrate spatially explicit winter survivorship estimates from a bioenergetic model of hibernation physiology. We apply this bioenergetic model given the presence of *P. destructans*, including parameters capturing its climate-dependent growth as well as its climate-dependent effects on host physiology, under both current climate conditions and scenarios of future climate change. We then update species distribution models with the resulting survivorship estimates to predict changes in winter hibernacula suitability under future conditions. Exposure to *P. destructans* is generally projected to decrease bats' winter occurrence probability, but in many areas, changes in climate are projected to lessen the detrimental impacts of WNS. This rescue effect is not predicted for all species or geographies and may arrive too late to benefit many hibernacula. However, our findings offer hope that proactive conservation strategies to minimize other sources of mortality could allow bat populations exposed to *P. destructans* to persist long enough for conditions to improve.

McClure, Meredith M.^{1*}, Hranac, Carter R.², Haase, Catherine G.^{3,4}, McGinnis, Seth⁵, Dickson, Brett G.^{1,6}, Hayman, David T.S.², McGuire, Liam P.^{7,8}, Lausen, Cori L.⁹, Plowright, Raina K.³, Fuller, N.^{7,10}, Olson, Sarah H.¹¹

¹ Conservation Science Partners, Truckee, USA

² ^mEpiLab, Hopkirk Research Institute, Massey University, Palmerston North, NZL

³ Department of Microbiology and Immunology, Montana State University, Bozeman, USA

⁴ Department of Biology, Austin Peay State University, Clarksville, USA

⁵ National Center for Atmospheric Research, Boulder, USA

⁶ Landscape Conservation Initiative, School of Earth and Sustainability, Northern Arizona University, Flagstaff, USA

⁷ Department of Biological Sciences, Texas Tech University, Lubbock, USA

⁸ Department of Biology, University of Waterloo, Waterloo, CAN

⁹ Wildlife Conservation Society Canada, Kaslo, CAN

¹⁰ Texas Parks & Wildlife Department, Austin, USA

¹¹ Wildlife Conservation Society, Health Program, Bronx, USA

***Corresponding author:** meredithlmclure@gmail.com

Keywords

Bats, subterranean microclimate, climate change, hibernation, species distribution model, white-nose syndrome

Introduction

Climate change and infectious disease emergence are major threats to biodiversity (Dawson et al. 2011, Fisher et al. 2012). Increasing temperatures, changes in the amount and timing of precipitation, increased frequency and severity of extreme conditions, and other changes in climate conditions (Pachauri et al. 2014) impact species and communities in a variety of ways. Climate change has already shifted distributions of a diverse range of species (Parmesan 2006) and is projected to drive future shifts (Lawler et al. 2009). Some species' fundamental niches are moving or disappearing altogether (Colwell & Rangel 2009, Thomas et al. 2004, Thuiller et al. 2006), while others may expand beyond range limits previously imposed by unsuitable climate conditions (e.g., Melles et al. 2011, Battisti & Larsson 2015). These range shifts may in turn drive changes in interspecific co-occurrence and population dynamics among competitors, predators, and prey (e.g., Alexander et al. 2016, Urban et al. 2013) as well as diseases, parasites, and hosts (Gallana et al. 2013, Adlard et al. 2015, Metcalf et al. 2017).

All of these climate change impacts may be at play for bats and are expected to interact with the impacts of white-nose syndrome (WNS). WNS, caused by a cold-loving fungus (*Pseudogymnoascus destructans*) introduced to New York state in 2006, has killed millions of hibernating bats across eastern and central North America by disrupting hibernation physiology (Leopardi et al. 2015, Frick et al. 2016). It continues to spread widely and rapidly from its introduction site, including a 2016 novel introduction to Washington state (USFWS 2020), and is now invading western North America (herein the West). *P. destructans* grows on the skin of hibernating bats and, through a number of physiological mechanisms, causes them to arouse from their torpid state more frequently than healthy bats (Frick et al. 2016). These arousals are energetically expensive (Thomas et al. 1990), causing infected bats to expend fat stores before the end of winter. Impact severity varies geographically and among species, and has been linked to microclimate-dependent fungal growth (Verant et al. 2012, Marroquin et al. 2017), interspecific and microclimate-dependent differences in host physiology (Johnson et al. 2014, Moore et al. 2017, McGuire et al. in review), as well as interspecific differences in hibernation behavior, including microclimate preferences (Langwig et al. 2012, 2016).

Despite the growing understanding of these mechanisms, WNS impacts on bats remain difficult to predict, particularly as *P. destructans* spreads to novel environments supporting diverse species (Harvey et al. 2013). For example, it is common to find large aggregations of hibernating bats in eastern and central North America, but this is rarely observed in the West. Instead, western bats tend to hibernate in widely distributed small groups (Weller et al. 2018, Adams 2003, Bachen et al. 2018). These differences, along with the rugged, remote landscapes characterizing much of the West, have made the study of western bats challenging. Gaps therefore remain in our understanding of western bat ecology and the potential impacts of various stressors, including continued WNS spread.

Climate change presents an additional layer of uncertainty regarding WNS impacts on bats. Bat hibernation physiology and behavior, as well as *P. destructans* physiology, are closely linked to climate conditions. Hibernaculum temperature and humidity, along with winter duration, dictate healthy hibernating bats' success in surviving winter on their fat stores (Thomas et al., 1990, Speakman & Thomas, 2003); temperature and humidity also determine fungal growth rates (Verant et al. 2012, Marroquin et al. 2017). WNS survivorship largely depends on whether fat stores can sustain bats through winter given increased arousal frequencies and associated energy costs resulting from *P. destructans* infection (Langwig et al. 2012, 2016, Hayman et al. 2016, Haase et al. 2019). A warming climate may shift bats' winter distributions to track shifts in preferred hibernaculum conditions. In some hibernacula, higher temperatures may increase fungal loads by expanding availability of suitable growth conditions, while other hibernacula may experience the opposite trend. These warming temperatures may simultaneously alter bats' winter energy expenditures, to their benefit or detriment. Meanwhile, shorter winters could help to reduce mortality resulting from infected bats expending fat stores too quickly.

We modeled current winter distributions of five bat species using a hybrid correlative-mechanistic approach (McClure et al. accepted; Fig. 1). We correlated observed winter occurrence of our focal species with landscape attributes expected to influence hibernaculum selection (e.g., topography, vegetation cover, water availability). As an additional predictor, we integrated a spatially explicit estimate of hibernation survivorship derived from a mechanistic bioenergetic model (Haase et al. 2019, Hranac et al. accepted). The bioenergetic model uses the hypothesized energetic requirements of bats during hibernation to dynamically model energy expenditure for the duration of a predicted winter under specified hibernaculum conditions. The model was parameterized for each of our focal species using field measurements of key aspects of hibernation physiology, and was run under current climate conditions, including model-based estimates of mean winter ambient temperatures experienced in hibernacula (McClure et al. 2020) and winter duration at a given location (Hranac et al. accepted).

Here, we apply this bioenergetic model given the presence of *P. destructans* : we include parameters capturing *P. destructans*' climate-dependent growth as well as its climate-dependent effects on host physiology, under both current climate conditions and scenarios of future climate change (Fig. 1). We then update our species distribution models (McClure et al. accepted) with the resulting survivorship estimates to predict changes in the distribution of suitable winter hibernacula under these projected future conditions. To our knowledge, there has been no attempt to model changing distributions of winter hibernacula in response to WNS exposure or climate change, let alone both. Our objective is to understand and predict the individual and joint effects of these two imminent stressors on North American bat populations. Our goal is to support researchers and managers in anticipating and planning for future impacts to bats. We expect this work will support managers in identifying species and geographies that are expected to be most affected by WNS, identifying populations for which WNS impacts may be either exacerbated or mitigated by climate change, and allocating monitoring and management resources accordingly.

Methods

We sought to estimate the change in five focal bat species' probability of occurrence (estimated under current conditions in McClure et al. accepted) given two future scenarios: a) exposure to *P. destructans*, and b) exposure to *P. destructans* and climate change. These species, including *Corynorhinus townsendii*, *Myotis californicus*, *M. lucifugus*, *M. velifer*, and *Perimyotis subflavus*, were selected based on data availability and representation of diverse distributions and habitat requirements among hibernating bats. To estimate bats' probability of occurrence given exposure to *P. destructans*, we ran the spatial bioenergetic model described in Hranac et al. (accepted; also see Haase et al. 2019) to project winter survivorship from parameters capturing the influence of the hibernaculum environment (temperature and humidity) on fungal growth and the resulting impact of the fungus on bat hibernation physiology. To estimate bats' probability of occurrence given the additional impacts of climate change, we ran the bioenergetic model with the *P. destructans* growth parameters above as well as projected future climate parameters (winter duration and

‘best available’ temperatures, identified as the subterranean temperature closest to the species’ preferred temperature as identified from published literature that was projected to be available in a given location; Fig. 1). The bioenergetic model, *P. destructans* growth parameters, and spatial application of the model are described fully in Haase et al. (2019) and Hranac et al. (accepted) and summarized in Appendix 1. We therefore focus here on describing integration of future climate scenarios into the bioenergetic model and subsequently SDMs for our five focal species.

We first projected daily temperatures at midcentury (2050) under a range of possible climate futures at high spatial resolution (1 km), which were then used to derive our climate parameters of interest. Global circulation models (GCMs) represent the energy budget of the earth system and the impact of external factors such as solar input and greenhouse gas emissions, simulating global patterns and processes across the earth’s major climate system components (atmosphere, ocean, sea ice, and land surface) to project future climate attributes (e.g., temperature, precipitation) under possible future scenarios of carbon and other heat-trapping gas concentrations (Kiel & Ramanathan 2006). regional climate models (RCMs) dynamically (i.e., mechanistically) downscale coarse GCM projections by resolving processes that occur at finer resolutions than GCM grid sizes (>100 km) within a more limited geographic scope (Kotamarthi et al. 2016). They account for the effects of local complexity, e.g., topography and coastlines, and simulate hydrologic processes at scales more relevant to decision-making (25-50 km). However, these outputs are still too coarse for many applications. GCM and RCM projections can be further statistically downscaled using a variety of approaches. Although many methods exist and vary considerably in their complexity, they all fundamentally aim to account for differences between model simulations applied to historical periods and observed climate attributes during those periods, then apply those statistical adjustments to future projections (Kotamarthi et al. 2016).

The NA-CORDEX Program data archive (Mearns et al. 2017), hosted by the National Center for Atmospheric Research, contains output from RCMs run over a domain covering most of North America using boundary conditions from multiple CMIP5 GCMs (Appendix 2, Fig. A1). These projections span a range of possible climate futures in terms of greenhouse gas concentration scenarios and projected severity of future change, as well as performance in capturing regionally important drivers and processes.

The NA-CORDEX data archive includes outputs from two RCMs that offer 25 km spatial resolution and span the complete range (2.4 - 4.6°C) of GCM equilibrium climate sensitivity (ECS), an emergent property of GCMs that serves as a metric of relative severity of projected change. These are the RegCM4 model (Giorgi et al. 2012) and the WRF model (Skamarock et al. 2008) (Fig. 2). These models differ in their underlying sub-models and -processes (see <https://na-cordex.org/rcm-characteristics>), which may mean that each best represents the meteorological phenomena driving future climate change in different subregions of North America. Kotamarthi et al. (2016) suggest that it is critical to understand the phenomena that are most relevant to climate impacts of interest when selecting the most appropriate downscaling tool. In the Mountain West, complex terrain is the primary driver of climate, with midlatitude cyclones, katabatic winds, monsoons, and associated air-mass thunderstorms being the most prominent resulting phenomena. The maritime climate along the Pacific coast also produces midlatitude cyclones, as well as orographic lifting and atmospheric rivers (Kotamarthi et al. 2016).

For each of the above RCMs, we selected downscaled outputs run on boundary conditions from two GCMs - GFDL-ESM2M (ECS = 2.4°C) and HadGEM2-ES (ECS = 4.6°C) - to span the range of available models’ climate sensitivity (Appendix 2, Fig. A1). This approach is in keeping with the recommendation from Kotamarthi et al. (2016) to use output from multiple GCMs with different physical parameterizations to cover a broader range of model uncertainty. Thus, in total, we consider four possible climate futures (2 RCMs x 2 GCMs).

We used versions of these outputs that were bias-corrected using a multivariate quantile mapping method (MBCn; Cannon 2018) with Daymet temperatures as the observed dataset (Thornton et al. 2019). Because the dynamically downscaled RCMs were still considerably coarser (25 km) than our desired spatial resolution (1 km), we further statistically downscaled them by spatially interpolating the data to 1 km and applying

an adiabatic lapse rate correction based on elevation (Wallace & Hobbs 2006).

To estimate survivorship under future conditions, we first derived 30-year means centered on the year 2050 for mean annual surface temperature (MAST) and duration of the frost-free period for each of the four climate scenarios. We then used projected MAST and a model linking surface and subterranean temperatures (McClure et al. 2020) to estimate the best available hibernaculum temperature likely to be available (i.e., the temperature closest to the mean ambient temperature at which each species has been observed during hibernation in the published literature) in any given location for a given species (see Appendix 1 for details). Similarly, projected frost-free period was used to estimate hibernation-specific winter duration (i.e., time between immergence and emergence from hibernacula) as described in Hranac et al. (accepted; also see Appendix 1). We then ran the bioenergetic survivorship model for each of our five focal species under each future scenario using these projected future climate parameters.

Projections of future winter survivorship under each scenario were then used as predictors in species-specific SDMs that were previously derived under current conditions. These SDMs are fully described in McClure et al. (accepted), but briefly, we brought model-based, spatially-explicit estimates of winter survivorship together with landscape attributes hypothesized to influence hibernaculum selection (e.g., topography, precipitation, presence of karst and mines) as predictors of relative probability of occurrence throughout the states and territories encompassing each species' known range (National Atlas of the United States 2011). We used boosted regression trees (Elith et al. 2008) to link these predictors to our response data, which consisted of species occurrence records compiled from multiple sources (e.g., online databases of museum records and vetted observations, Natural Heritage Programs, our own field studies). The influence of each predictor on final predictive models for each species are summarized in Fig. 2. We then applied the final model for each species to predictor values in each 1-km cell to predict and map relative probability of occurrence. Here, we essentially updated these models by replacing survivorship estimates under current conditions with projected survivorship under future scenarios. We then estimated and mapped the change in occurrence probability between current conditions and each future scenario as the difference in estimated occurrence probability for each raster cell.

Results & Discussion

Mean projected climate parameters (MAST and frost-free period) among the four climate scenarios assessed are mapped in Fig. 3, along with the inter-scenario range and the mean projected change in each parameter from current conditions. Spatial patterns in the mean parameter values reflect latitudinal, topographic, and coastal influences on temperature and frost-free period, as expected. We observed high agreement among climate scenarios (i.e., low inter-scenario range) for projected MAST, with increasing disagreement at very high latitudes. Disagreement among climate scenarios in length of the frost-free period was higher in some areas and more sporadic than that seen in MAST projections, which may reflect a stronger influence of topography. Projected change in MAST increased with latitude and with elevation, while projected change in frost-free period was more spatially variable, with the largest increases in the Appalachian region and localized portions of the West coast.

Projected changes in probability of occurrence for each of five focal species under future scenarios are mapped in Figs. 4-6 and Figs. A2-A3 (Appendix 2). We focus on projections from SDMs in which the survivorship predictor accounted for at least 5% of the boosted regression tree model fit under current conditions (McClure et al. accepted; Fig. 2), which included models for *M. californicus*, *M. lucifugus*, and *P. subflavus*. Projections from SDMs to which survivorship contributed less than 5% (*C. townsendii*, *M. velifer*) are expected to be less useful because little clear relationship between known species occurrences and survivorship emerged.

Generally, probability of occurrence was projected to decline following exposure to *P. destructans* (with the exception of *C. townsendii*, Appendix 2, Fig. A2). However, projected occurrence probability increased for most species in most places when climate change was also considered. The greatest projected declines with *P. destructans* exposure were typically in areas with the highest occurrence probability under current

conditions (i.e., the areas currently expected to be most suitable for a given species). Spatial patterns in change in occurrence probability after considering climate impacts were more variable. For *M. californicus*, we projected moderate declines in occurrence probability in British Columbia, but a strong increase in other high occurrence probability portions of the range (Fig. 4). For *M. lucifugus*, we projected decreases in the severity of declines, but climate change had little impact on areas already expected to remain stable or experience increased occurrence probability (Fig. 5). In contrast, we observed thresholding behavior in *P. subflavus* such that projected rangewide declines under *P. destructans* exposure were replaced by a marked increase in occurrence probability in the southeast given climate change (Fig. 6). This threshold appears to follow and is thus probably driven by spatial patterns in the frost-free period (Fig. 3). We do not interpret projected changes under each future scenario for *C. townsendii* or *M. velifer* because the low contribution of winter survivorship estimates to SDM fits appear to result in unreliable and counterintuitive behavior of models for these species (Appendix 2, Figs. A2-A3).

It may be important to consider patterns in projected changes in occurrence probability not just across the known range of each species, but also more specifically at known hibernacula. We summarized projected changes in relative probability of occurrence at the points of winter capture or observation that informed development of species distribution models (Table 1). For *M. californicus* and *P. subflavus*, the vast majority of winter locations are projected to exhibit decreased occurrence probability with exposure to WNS (92.6 and 98.9% of locations, respectively), but climate change scenarios reduce these figures to 43.2 and 65.3%, respectively, on average. Thus, although climate change is projected to significantly mitigate the impacts of WNS on these species, approximately half of known hibernaculum locations may still experience declines in occurrence. In the case of *M. lucifugus*, WNS exposure is projected to result in decreased occurrence probability at 41.2% of winter locations, and climate change is anticipated to have little effect on this pattern (projected declines at 43.1% of locations, on average).

All four climate scenarios showed close agreement regarding future changes in occurrence probability. This agreement may be driven by one or more factors. First, derived estimates of MAST and frost-free period may not be sensitive to differences among scenarios in projected daily temperatures. This appears to be more likely for MAST than for frost-free period (Fig. 3) and is not surprising given that calculation of the frost-free period is threshold dependent (i.e., definition of the frost-free period is dependent on the first and last day of the year on which a precise threshold temperature is reached). Second, the subterranean temperature model and/or winter duration model may not be sensitive to MAST and frost-free period parameters, respectively (see Fig. 1). This is unlikely in the case of the subterranean temperature model, given that MAST is the model's strongest predictor (McClure et al. 2020). It is also unlikely in the case of the winter duration model given that inclusion of frost-free period as a predictor improved the model by 25.39 AIC units (Hranac et al. accepted). Third, the survivorship model may not be sensitive to variation in the best available temperature estimate derived from the subterranean temperature model and/or our estimate of winter duration. We suggest that derivation of the 'best available' temperature for a given species at a given location from the subterranean temperature model likely absorbs the majority of the variability among climate scenarios (see Appendix 1, Hranac et al. accepted). Finally, for some species, SDMs may not be sensitive to variation in winter survivorship estimates. SDM sensitivity to survivorship is expected to be directly related to the contribution of the survivorship predictor to the boosted regression tree model for a given species (see McClure et al. accepted).

Although all climate scenarios produced very similar projections of future change in occurrence probability, differences were apparent in some places for most species. For *M. californicus*, differences were most apparent along the Pacific coast near the California-Oregon border and around the state of Oklahoma (Fig. 4). For *P. subflavus*, the location of the threshold between increasing and decreasing occurrence probability fluctuated across the Appalachian region among scenarios (Fig. 6). Model disagreement was also evident in Oklahoma for *C. townsendii* and *M. velifer*, as well as the Columbia Plateau of eastern Washington and the Sierra Nevada range of California, respectively (Appendix 2, Figs. A2-A3).

We suggest that our predictions of species distributions in the presence of *P. destructans* and future climate

conditions can help managers to better anticipate the species- and place-specific impacts of these stressors, individually and synergistically, across North America. Our results may inform on-the-ground monitoring, which will be important for efforts to track trends in bat distribution and abundance, such as the North American Bat Monitoring Program (Loeb et al. 2015). Our results may help to inform placement of passive acoustic detectors for monitoring as *P. destructans* continues to spread and the climate continues to warm. For example, monitoring of bat populations could be targeted in areas where our projections suggest that suitable hibernation conditions are likely to be lost and that occurrence probability is likely to decline (vulnerable hibernacula). Conversely, monitoring as well as protection efforts could target hibernacula that are likely to be retained (potential refugia). Our predictions may also enable assessment of the distribution of at-risk and stable hibernacula across federal, state, and private lands to guide engagement strategies for conservation. Additionally, they may help managers to prepare for possible range expansions into or contractions from their jurisdictions under future climate conditions.

Our findings suggest that by mid-century, changing temperatures may offer a ‘rescue’ effect for many bat populations from the deleterious effects of *P. destructans*. However, given the pace of *P. destructans*’ spread from the East and its recent detection in New Mexico and Montana (USFWS 2020), this rescue effect may arrive too late for many hibernacula. Furthermore, a warming climate is not predicted to shield all species in all areas (e.g., *M. californicus* in British Columbia, *M. lucifugus* in mountainous regions, *P. subflavus* in the northeastern United States), and climate change may have other deleterious impacts on bats that are beyond the scope of our models (e.g., increasing aridity, driving declines in insect populations). It is therefore important that managers continue to strive for effective proactive conservation strategies to combat the devastating impacts of *P. destructans* as the fungus continues to spread. Even in the absence of a ‘cure’ for WNS, conservation and management actions that minimize other sources of mortality may allow bat populations to persist long enough for conditions to improve.

Acknowledgements

This project has been funded in part with Federal funds from the Department of Defense Environmental Research and Development Program (SERDP), under Contract Number W912HQ-16-C-0015. DTSH is funded by Royal Society Te Aparangi, grant number MAU1701. We are grateful to Linda Mearns for input on appropriate selection and application of projected climate data. We thank Nathan Justice, Eric Stofferahn, and Tony Chang for valuable technical support. Finally, we are indebted to the many individuals and organizations who generously provided raw data that made possible the studies supporting this paper, including subterranean microclimate data, bat species occurrence locations, hibernaculum immergence and emergence observations, and bat physiology records (see Haase et al. 2019, McClure et al. 2020, Hranac et al. accepted, and McClure et al. accepted for further details).

Required disclosure: Any opinions, findings, and conclusions or recommendations expressed in this publication are those of the author(s) and do not necessarily reflect the views of the Government.

Literature Cited

- Adlard, R.D., Miller, T.L. and Smit, N.J., 2015. The butterfly effect: parasite diversity, environment, and emerging disease in aquatic wildlife. *Trends in Parasitology*, 31(4), pp.160-166.
- Alexander, J.M., Diez, J.M., Hart, S.P. and Levine, J.M., 2016. When climate reshuffles competitors: a call for experimental macroecology. *Trends in Ecology & Evolution*, 31(11), pp.831-841.
- Battisti, A. and Larsson, S., 2015. Climate change and insect pest distribution range. *Climate Change and Insect Pests*. CABI, Wallingford, pp.1-15.
- Cannon, A.J., 2018. Multivariate quantile mapping bias correction: an N-dimensional probability density function transform for climate model simulations of multiple variables. *Climate dynamics*, 50(1-2), pp.31-49.

- Colwell, R.K. and Rangel, T.F., 2009. Hutchinson's duality: the once and future niche. *Proceedings of the National Academy of Sciences*, 106(Supplement 2), pp.19651-19658.
- Dawson, T.P., Jackson, S.T., House, J.I., Prentice, I.C. and Mace, G.M., 2011. Beyond predictions: biodiversity conservation in a changing climate. *Science*, 332(6025), pp.53-58.
- Fisher, M.C., Henk, D.A., Briggs, C.J., Brownstein, J.S., Madoff, L.C., McCraw, S.L. and Gurr, S.J., 2012. Emerging fungal threats to animal, plant and ecosystem health. *Nature*, 484(7393), pp.186-194.
- Frick, W.F., Puechmaille, S.J. and Willis, C.K., 2016. White-nose syndrome in bats. In *Bats in the Anthropocene: Conservation of bats in a changing world* (pp. 245-262). Springer, Cham.
- Gallana, M., Ryser-Degiorgis, M.P., Wahli, T. and Segner, H., 2013. Climate change and infectious diseases of wildlife: altered interactions between pathogens, vectors and hosts. *Current Zoology*, 59(3), pp.427-437.
- Giorgi, F., E. Coppola, F. Solmon, L. Mariotti, M.B. Sylla, X. Bi, N. Elguindi, G.T. Diro, V. Nair, G. Giuliani, U.U. Turuncoglu. 2012. RegCM4: model description and preliminary tests over multiple CORDEX domains. *Climate Research* 52: 7-29.
- Haase, C.G., Fuller, N.W., Hranac, C.R., Hayman, D.T., McGuire, L.P., Norquay, K.J., Silas, K.A., Willis, C.K., Plowright, R.K. and Olson, S.H., 2019. Incorporating evaporative water loss into bioenergetic models of hibernation to test for relative influence of host and pathogen traits on white-nose syndrome. *PLoS one*, 14(10), p.e0222311.
- Harvey, M.J., Altenbach, J.S., & Best, T.L. (2013). *Bats of the United States and Canada*. Johns Hopkins University Press.
- Johnson, J.S., Reeder, D.M., McMichael III, J.W., Meierhofer, M.B., Stern, D.W., Lumadue, S.S., Sigler, L.E., Winters, H.D., Vodzak, M.E., Kurta, A. and Kath, J.A., 2014. Host, pathogen, and environmental characteristics predict white-nose syndrome mortality in captive little brown myotis (*Myotis lucifugus*). *PLoS One*, 9(11), p.e112502.
- Kiehl, J.T. and Ramanathan, V. eds., 2006. *Frontiers of climate modeling*. Cambridge University Press.
- Kotamarthi, R., L. Mearns, K. Hayhoe, C. Castro, D. Wuebbles. 2016. Use of climate information for decision-making and impacts research: state of our understanding. Prepared for the Department of Defense, Strategic Environmental Research and Development Program. 55pp.
- Langwig, K.E., Frick, W.F., Hoyt, J.R., Parise, K.L., Drees, K.P., Kunz, T.H., Foster, J.T. and Kilpatrick, A.M., 2016. Drivers of variation in species impacts for a multi-host fungal disease of bats. *Philosophical Transactions of the Royal Society B: Biological Sciences*, 371(1709), p.20150456.
- Langwig, K.E., Frick, W.F., Bried, J.T., Hicks, A.C., Kunz, T.H. and Marm Kilpatrick, A., 2012. Sociality, density-dependence and microclimates determine the persistence of populations suffering from a novel fungal disease, white-nose syndrome. *Ecology letters*, 15(9), pp.1050-1057.
- Lawler, J.J., Shafer, S.L., White, D., Kareiva, P., Maurer, E.P., Blaustein, A.R. and Bartlein, P.J., 2009. Projected climate-induced faunal change in the Western Hemisphere. *Ecology*, 90(3), pp.588-597.
- Leopardi, S., Blake, D. and Puechmaille, S.J., 2015. White-nose syndrome fungus introduced from Europe to North America. *Current Biology*, 25(6), pp.R217-R219.
- Loarie, S.R., Duffy, P.B., Hamilton, H., Asner, G.P., Field, C.B. and Ackerly, D.D., 2009. The velocity of climate change. *Nature*, 462(7276), pp.1052-1055.
- Marroquin, C.M., Lavine, J.O. and Windstam, S.T., 2017. Effect of humidity on development of *Pseudogymnoascus destructans*, the causal agent of bat white-nose syndrome. *Northeastern Naturalist*, 24(1), pp.54-64.

- McClure, M.L., Crowley, D., Haase, C.G., McGuire, L.P., Fuller, N.W., Hayman, D.T.S., Lausen, C.L., Plowright, R.K. Dickson, B.G. and Olson S.H. 2020. Linking surface and subterranean climate: implications for the study of hibernating bats and other cave dwellers. *Ecosphere* 11(10):e03274.
- Mearns, L.O., et al. 2017. The NA-CORDEX dataset, version 1.0. NCAR Climate Data Gateway, Boulder CO. <https://doi.org/10.5065/D6SJ1JCH>
- Melles, S.J., Fortin, M.J., Lindsay, K. and Badzinski, D., 2011. Expanding northward: influence of climate change, forest connectivity, and population processes on a threatened species' range shift. *Global Change Biology*, 17(1), pp.17-31.
- Metcalf, C.J.E., Walter, K.S., Wesolowski, A., Buckee, C.O., Shevliakova, E., Tatem, A.J., Boos, W.R., Weinberger, D.M. and Pitzer, V.E., 2017. Identifying climate drivers of infectious disease dynamics: recent advances and challenges ahead. *Proceedings of the Royal Society B: Biological Sciences*, 284(1860), p.20170901.
- Mitchell, T.D., P.D. Jones. 2005. An improved method of constructing a database of monthly climate observations and associated high-resolution grids. *International Journal of Climatology* 25:693–712.
- Moore, M.S., Field, K.A., Behr, M.J., Turner, G.G., Furze, M.E., Stern, D.W., Allegra, P.R., Bouboulis, S.A., Musante, C.D., Vodzak, M.E. and Biron, M.E., 2018. Energy conserving thermoregulatory patterns and lower disease severity in a bat resistant to the impacts of white-nose syndrome. *Journal of Comparative Physiology B*, 188(1), pp.163-176.
- National Atlas of the United States, 2011. North American Bat Ranges. National Atlas of the United States, Reston, Virginia. Available: <https://www.sciencebase.gov/catalog/item/4f4e4814e4b07f02db4dab2e>
- Opdam, P. and Wascher, D., 2004. Climate change meets habitat fragmentation: linking landscape and biogeographical scale levels in research and conservation. *Biological conservation*, 117(3), pp.285-297.
- Pachauri, R.K., Allen, M.R., Barros, V.R., Broome, J., Cramer, W., Christ, R., Church, J.A., Clarke, L., Dahe, Q., Dasgupta, P. and Dubash, N.K., 2014. Climate change 2014: synthesis report. Contribution of Working Groups I, II and III to the fifth assessment report of the Intergovernmental Panel on Climate Change. IPCC.
- Parmesan, C., 2006. Ecological and evolutionary responses to recent climate change. *Annu. Rev. Ecol. Evol. Syst.*, 37, pp.637-669.
- Reeder, D.M., Frank, C.L., Turner, G.G., Meteyer, C.U., Kurta, A., Britzke, E.R., Vodzak, M.E., Darling, S.R., Stihler, C.W., Hicks, A.C. and Jacob, R., 2012. Frequent arousal from hibernation linked to severity of infection and mortality in bats with white-nose syndrome. *PLoS One*, 7(6), p.e38920.
- Skamarock, W.C., J.B. Klemp, J. Dudhia, D.O. Gill, D.M. Barker, M.G. Duda, X. Huang, W. Wang, J.G. Powers. 2008. A Description of the Advanced Research WRF Version 3. NCAR Technical Note NCAR/TN-475+STR. 125pp.
- Thomas, D.W., Dorais, M. and Bergeron, J.M., 1990. Winter energy budgets and cost of arousals for hibernating little brown bats, *Myotis lucifugus*. *Journal of mammalogy*, 71(3), pp.475-479.
- Thomas, C.D., Cameron, A., Green, R.E., Bakkenes, M., Beaumont, L.J., Collingham, Y.C., Erasmus, B.F., De Siqueira, M.F., Grainger, A., Hannah, L. and Hughes, L., 2004. Extinction risk from climate change. *Nature*, 427(6970), pp.145-148.
- Thornton, P.E., Thornton, M.M., Mayer, B.W., Wei, Y., Devarakonda, R., Vose, R.S., and Cook, R.B., 2019. Daymet: Daily Surface Weather Data on a 1-km Grid for North America, Version 3. ORNL DAAC, Oak Ridge, Tennessee, USA.
- Thuiller, W., Lavorel, S., Araujo, M.B., Sykes, M.T. and Prentice, I.C., 2005. Climate change threats to plant diversity in Europe. *Proceedings of the National Academy of Sciences*, 102(23), pp.8245-8250.

Travis, J.M.J., 2003. Climate change and habitat destruction: a deadly anthropogenic cocktail. Proceedings of the Royal Society of London. Series B: Biological Sciences, 270(1514), pp.467-473.

United States Fish & Wildlife Service. 2020. Whitenosesyndrome.org. A coordinated response to devastating bat disease. Available: <https://www.whitenosesyndrome.org>.

Urban, M.C., Zarnetske, P.L. and Skelly, D.K., 2013. Moving forward: dispersal and species interactions determine biotic responses to climate change. Annals of the New York Academy of Sciences, 1297(1), pp.44-60.

Verant, M.L., Boyles, J.G., Waldrep Jr, W., Wibbelt, G. and Blehert, D.S., 2012. Temperature-dependent growth of *Geomyces destructans*, the fungus that causes bat white-nose syndrome. PloS one, 7(9), p.e46280.

Wallace, J.M. and Hobbs, P.V., 2006. Atmospheric science: an introductory survey (Vol. 92). Elsevier.

Tables

Table 1. Percent of points of winter capture/observation for each of five focal species that are projected to exhibit decreased relative probability of occurrence following exposure to WNS and climate change. Future climate scenarios were driven by each combination of two global circulation models (GCMs): GFDL-ESM2M (Scenarios 1, 2) and HadGEM2-ES (Scenarios 3, 4) and two dynamically-downscaled regional climate models (RCMs): RegCM4 (Scenarios 1, 3) and WRF (Scenarios 2, 4).

Species	n locations	Percent locations with projected decrease in Pr(Occ)				
		WNS	WNS + Scenario 1	WNS + Scenario 2	WNS + Scenario 3	WNS + Scenario 4
<i>M. californicus</i>	95	92.6	44.2	45.3	41.1	42.1
<i>M. lucifugus</i>	442	41.2	41.4	43.0	42.1	45.9
<i>P. subflavus</i>	284	98.9	77.1	58.1	73.2	52.8
<i>C. townsendii</i>	355	45.6	61.1	65.6	64.2	66.2
<i>M. velifer</i>	72	90.3	79.2	50.0	75.0	62.5

Figures

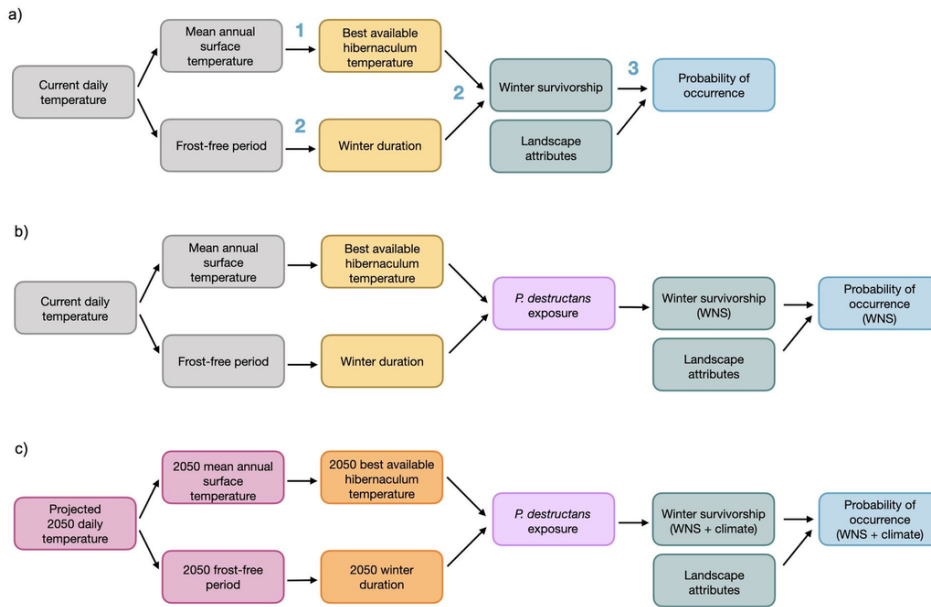


Figure 1. Flowchart schematic detailing steps in development of species distribution models (SDMs) for five focal bat species under a) current conditions, b) exposure to *P. destructans*, and c) exposure to *P. destructans* and projected climate change. Numbered steps are those detailed in previous related publications that support the work presented here: 1) McClure et al. 2020, *Ecosphere*, 2) Hranac et al. accepted, *Ecology and Evolution*, and 3) McClure et al. accepted, *Journal of Biogeography*.

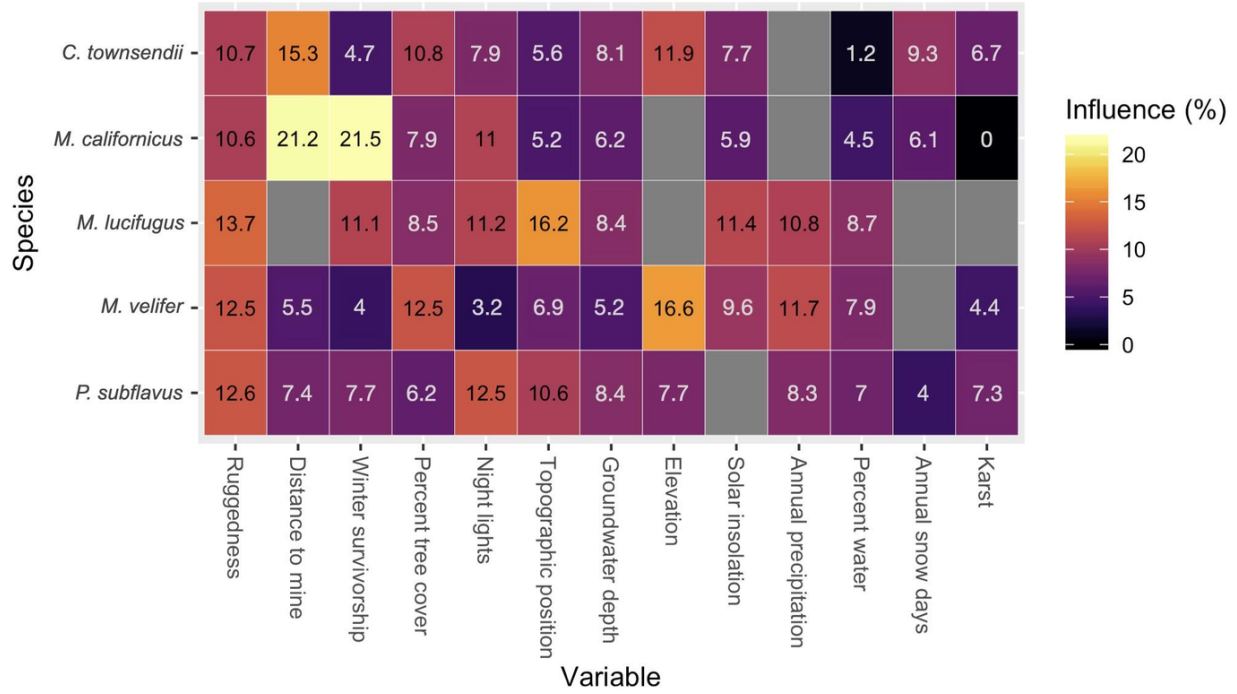


Figure 2. Final predictor influences in boosted regression tree models estimating winter species distributions of bat species *Corynorhinus townsendii*, *Myotis californicus*, *Myotis lucifugus*, *Myotis velifer*, and *Perimyotis subflavus* across the United States and Canada. Brighter colors indicate higher influence; predictors that were dropped from a given model are shown in gray. Variables are ordered by their average influence across species (decreasing left to right).

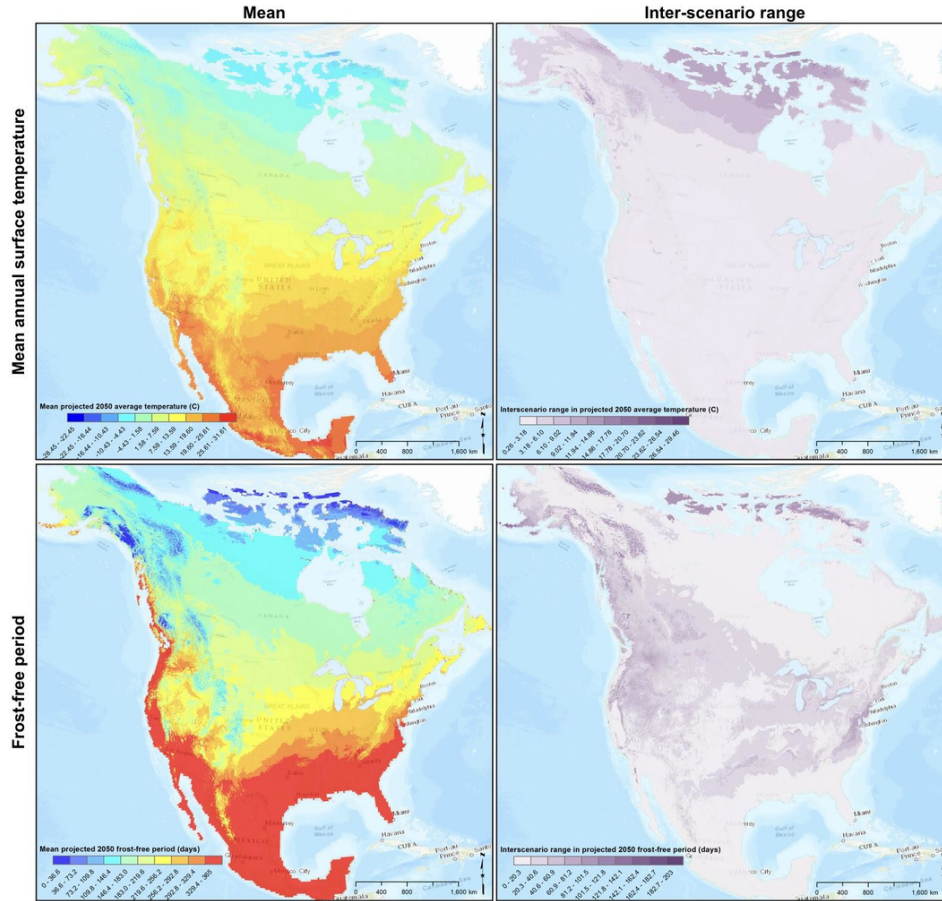


Figure 3. Projected mid-century climate conditions (30-year averages centered on 2050) used to parameterize bioenergetic survivorship models: mean annual surface temperature (left) and duration of frost-free period (right). Winter survivorship estimates were subsequently used as predictors of occurrence probability in species distribution models for five focal bat species. Future climate scenarios were driven by each combination of two global circulation models (GCMs): GFDL-ESM2M and HadGEM2-ES, and two dynamically-downscaled regional climate models (RCMs): RegCM4 and WRF. We show the mean (top) and range (center) among the four scenarios as well as the mean projected change from current conditions (bottom).

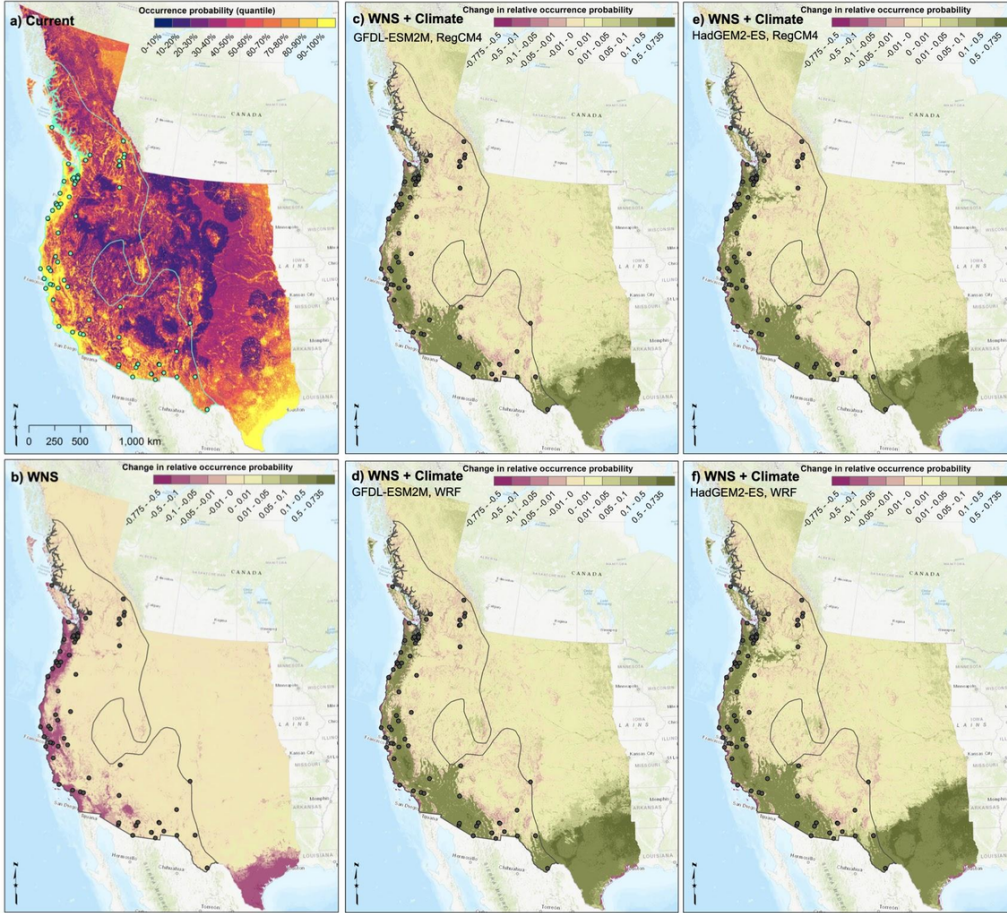


Figure 4. Projected change in *Myotis californicus* relative probability of occurrence (a) under multiple future scenarios: exposure to white-nose syndrome (WNS) under current climate conditions (b) and exposure to WNS under projected mid-century climate conditions (c-f). Future climate scenarios were driven by each combination of two global circulation models (GCMs): GFDL-ESM2M (c-d) and HadGEM2-ES (e-f) and two dynamically-downscaled regional climate models (RCMs): RegCM4 (c,e) and WRF (d,f). Darker green indicates a projected increase in occurrence probability; darker purple indicates a projected decrease. The species' current known range (gray outline) and points of winter captures/observations (gray points) are overlaid.

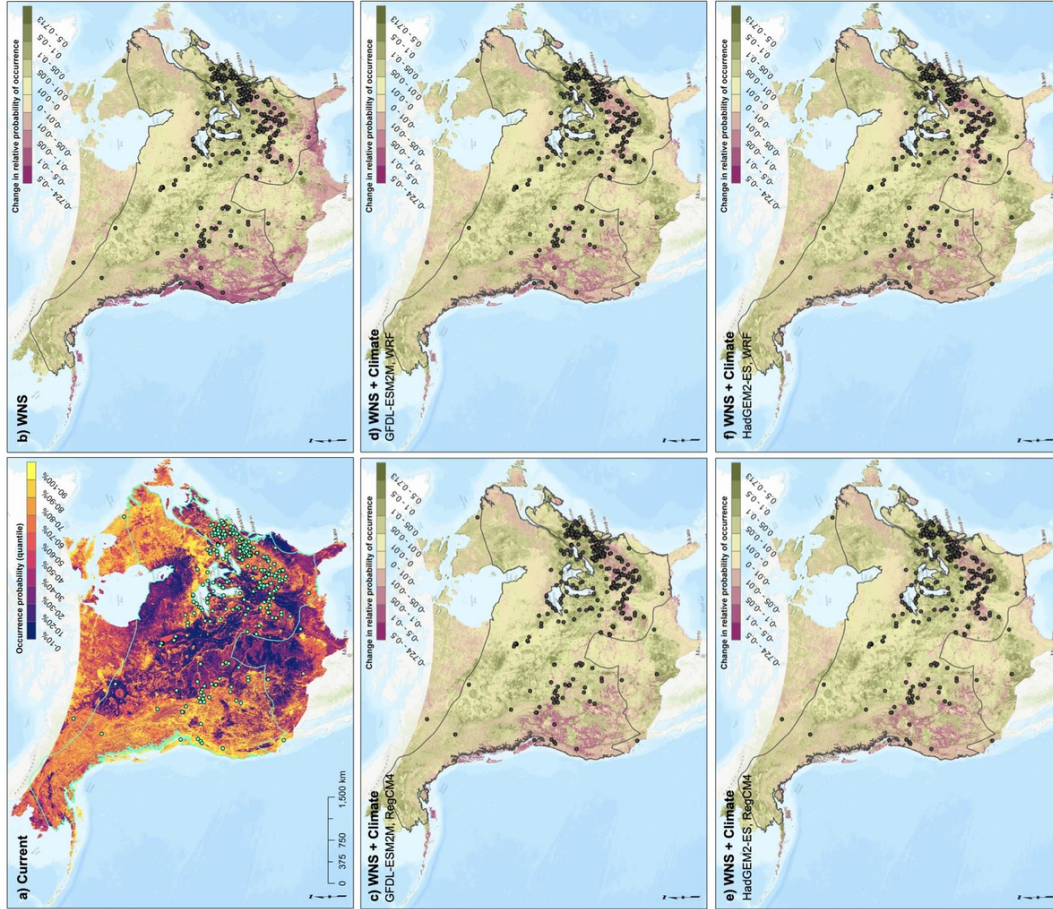


Figure 5. Projected change in *Myotis lucifugus* relative probability of occurrence (a) under multiple future scenarios: exposure to white-nose syndrome (WNS) under current climate conditions (b) and exposure to WNS under projected mid-century climate conditions (c-f). Future climate scenarios were driven by each combination of two global circulation models (GCMs): GFDL-ESM2M (c-d) and HadGEM2-ES (e-f) and two dynamically-downscaled regional climate models (RCMs): RegCM4 (c,e) and WRF (d,f). Darker green indicates a projected increase in occurrence probability; darker purple indicates a projected decrease. The species' current known range (gray outline) and points of winter observations/captures (gray points) are overlaid.

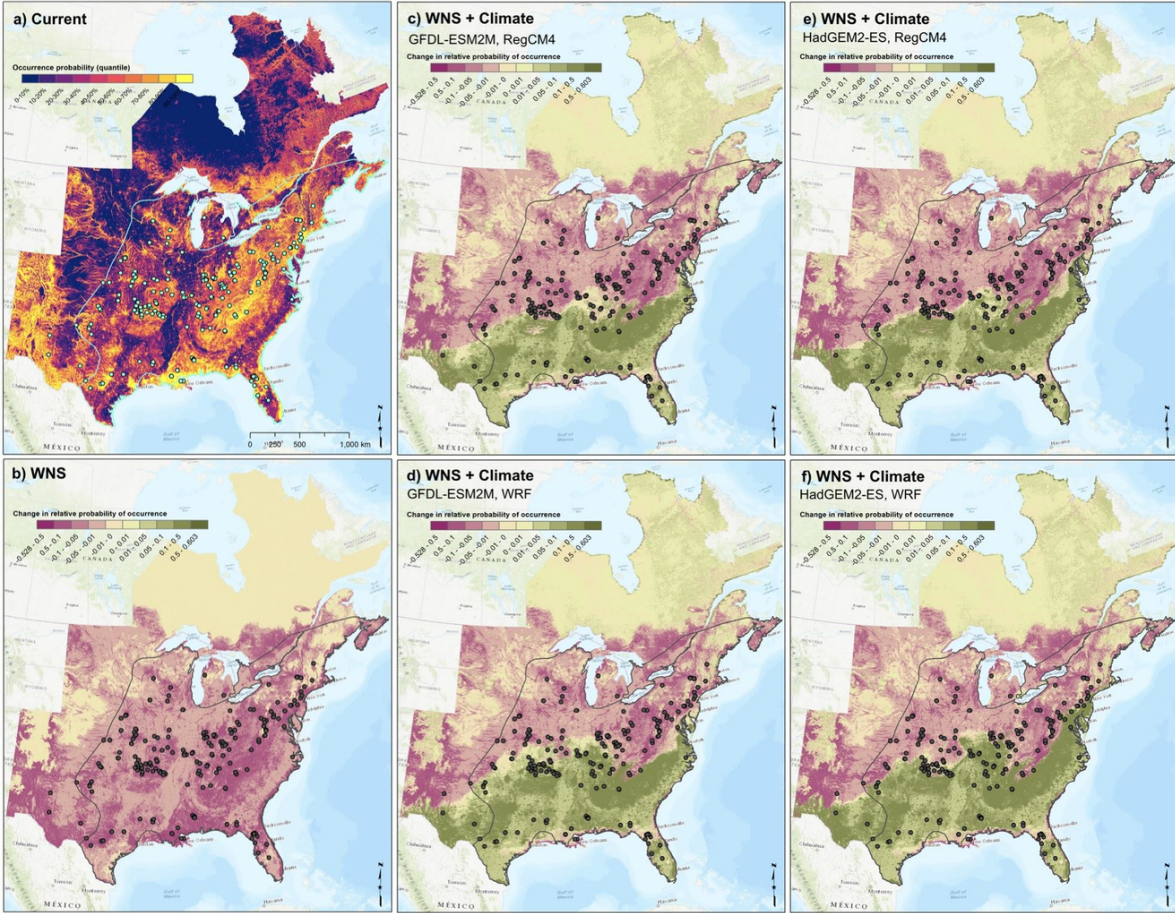


Figure 6. Projected change in *Perimyotis subflavus* relative probability of occurrence (a) under multiple future scenarios: exposure to white-nose syndrome (WNS) under current climate conditions (b) and exposure to WNS under projected mid-century climate conditions (c-f). Future climate scenarios were driven by each combination of two global circulation models (GCMs): GFDL-ESM2M (c-d) and HadGEM2-ES (e-f) and two dynamically-downscaled regional climate models (RCMs): RegCM4 (c,e) and WRF (d,f). Darker green indicates a projected increase in occurrence probability; darker purple indicates a projected decrease. The species' current known range (gray outline) and points of winter captures/observations (gray points) are overlaid.

Appendix 1: Winter survivorship model

Full details describing the hibernation energetic model structure and parameterization are described elsewhere (Haase et al. 2019, Hranac et al. accepted); here we provide a brief description and details regarding spatial application of the model across the study extent. The model uses the hypothesized energetic requirements of bats in torpor to dynamically model torpor bouts for the duration of a predicted winter under specified hibernation conditions. Specifically, ambient temperature and water loss are drivers of hibernating bats' arousal frequency over the course of the winter, which subsequently drives energy expenditure and fat loss. Likelihood of winter survivorship can be estimated based on the predicted fat mass remaining at the end of winter. Key parameters include bat morphometrics and metabolic rates, whether bats are infected with *P. destructans*, and hibernaculum climate conditions.

The model (as described in Haase et al. 2019) was applied for bats assumed to be uninfected with *P. destructans* using species-specific metabolic and morphometric parameter defaults contained with the batwintor R

package (in development: github.com/cReedHranac/batwintor). We then applied the resulting model at each 1-km² grid cell across the study extent using spatially explicit estimates of mean ambient temperatures and winter duration and a fixed relative humidity value of 95%.

Ambient temperature. Hibernating bats are understood to prefer and select particular temperatures from the range of temperatures that may be available within a given hibernaculum. As subterranean temperatures in caves and mines are known to deviate from mean annual surface temperature (MAST) due to a variety of factors (Perry 2013), we developed a model to predict the availability of suitable hibernacula temperatures (McClure et al. 2020).

We estimated the mean ambient temperature likely to be experienced over the course of hibernation in any given location across North America should a suitable hibernaculum exist, for each of our five focal species. We first identified the mean ambient temperature at which each species has been observed during hibernation from the available published literature (Table S1), and made the assumption that this mean represents the species’ preferred hibernation temperature. We then used a spatially explicit model of subterranean winter temperatures to estimate the closest available temperature to this preferred temperature at any given location (McClure et al. 2020). The model estimates subterranean winter temperature based on MAST, distance from the site entrance, site type (cave or mine), and several less influential predictors representing topography, land cover, and presence of water. The model predicts an increase in subterranean temperature with increasing MAST and distance from the site entrance, and predicts higher temperatures in mines than in caves.

We bracketed the conditions expected to be available at a given site by assuming, based on field observations, that bats would hibernate between 50 and 100 meters from the site entrance (except *C. townsendii*, which were assumed to hibernate between 10 and 100 meters from the site entrance) (C. Lausen, personal communication). To estimate the warmest temperature potentially available at a given site, we predicted subterranean temperatures at 100 m from entrances of mines. To estimate the coldest temperature potentially available, we predicted subterranean temperatures at 50 m (10 m for *C. townsendii*) from entrances of caves. We then conditionally selected the best available temperature (i.e., the closest to the species-specific preferred temperature) for each raster cell across North America. Each cell was assigned the species’ preferred temperature if this temperature was bounded by the coldest and warmest temperature predicted to be available for that cell. If it was not, the cell was assigned the closest temperature to the preferred temperature that was predicted to be available. If the available range was too cold, the warmest available temperature (i.e., the predicted temperature for mines at 100 m) was assigned, and if the available range was too warm, the coldest available temperature (i.e., the predicted temperature for caves at 50 m/10 m) was assigned. For cells where the best available temperature differed from the parameterized optimal hibernacula temperature, the metabolic rate was scaled through the q10 relationship, as fully described in Haase et al. (2019) and Hayman et al. (2016). In all cases, deviation away from the parameterized temperature will increase the rate of metabolic expenditure. At the warmest of locations, bats may be unable to fully enter torpor and therefore require vastly more energy than a torpid individual to survive a hibernation duration of the same length.

This approach best captured our assumption that bats will select microsites within hibernacula that offer their preferred temperature when possible, but will likely tolerate warmer or cooler temperatures when necessary, especially at the margins of their ranges.

Table A1. Published literature containing observed ambient hibernaculum temperatures for focal species *C. townsendii*, *M. californicus*, *M. lucifugus*, *M. velifer*, and *P. subflavus* that were used to estimate preferred hibernation temperatures.

Species	Reference	State or province
<i>Corynorhinus macrotis</i>	Hahn, W.L. 1908. Indiana University, 95:135-164	IN
<i>Corynorhinus rafinesquii</i>	Dalquest, W.W. 1947. Journal of Mammalogy 28(1):17-30	CA
<i>Corynorhinus rafinesquii</i>	Layne, J.N. 1958. The American Midland Naturalist 60(1):219-254	IL
<i>Corynorhinus rafinesquii</i>	Pearson, etl al. 1952. Journal of Mammalogy 33(3):273-320	CA
<i>Corynorhinus rafinesquii</i>	Pearson, etl al. 1952. Journal of Mammalogy 33(3):273-320	CA
<i>Corynorhinus rafinesquii intermedius</i>	Gumderston, et al. 1944. Journal of Mammalogy 25(3):307-319	NV
<i>Corynorhinus rafinesquii intermedius</i>	Twente, J.W. 1955. Ecology 36(4):706-732	KS
<i>Corynorhinus townsendii</i>	Gillies, K.E. et al. 2014. Natural Areas Journal 34(1):24:30	ID
<i>Corynorhinus townsendii</i>	Hayes, M.A. et al. 2011. Journal of Wildlife Management 75(1):137-143	CO
<i>Corynorhinus townsendii</i>	Hurst, T.E. & Lacki M.J. 1999. The American Midland Naturalist 142 (2):363-371	KY
<i>Corynorhinus townsendii</i>	Ingersoll, T.E. et al. 2010. Journal of Mammalogy 91(5):1242-1250	CO
<i>Corynorhinus townsendii</i>	Lopez-Gonzalez & Torres-Morales 2004	MEX
<i>Corynorhinus townsendii ingens</i>	Clark, B.K. et al. 1996. Wildlife Society Bulletin 24(1):8-14	OK, KS
<i>Plecotus townsendii</i>	Hughes, S.E. 1968. Journal of Mammalogy 49(1):140-142	WA
<i>Plecotus townsendii</i>	Hughes, S.E. 1968. Journal of Mammalogy 49(1):140-142	WA
<i>Plecotus townsendii</i>	Humphrey, S.A. & Kunz, T.H. 1976. Journal of Mammalogy 57(3):470-494	OK
<i>Plecotus townsendii pallescens</i>	Martin, R.A. & Hawks B.G. 1972. Bull. New Jersey Acad. Sci 17(2):24-30	SD
<i>Myotis californicus</i>	Dalquest, W.W. 1947. Journal of Mammalogy 28(1):17:30	AR
<i>Myotis californicus</i>	Reeder, W.G. 1949. Journal of Mammalogy 30(1):51-53	TX
<i>Myotis lucifugus</i>	Boyles, J.G., et al. 2007. Journal of Experimental Biology 210(24):4345-4350	OH
<i>Myotis lucifugus</i>	Brack, V. 2007. Environmental Management 40(5):739-746	OH
<i>Myotis lucifugus</i>	Davis, W.H. & Hitchcock, H.B. 1964. Journal of Mammalogy 45(3):475-476	NY
<i>Myotis lucifugus</i>	Fenton, M.B. 1970. Royal Ontario Museum	ON
<i>Myotis lucifugus</i>	Henshaw, R.E. & Folk Jr, G.E. 1966. Physiological Zoology 39(3):223-236	KY
<i>Myotis lucifugus</i>	Hitchcock, H.B. 1949. Canadian Field-Naturalist 63(1):47-59	ON, QC
<i>Myotis lucifugus</i>	Jonasson, K.A. & Willis, C.K. 2012. Journal of Experimental Biology 215 (12):2141-2149	MB
<i>Myotis lucifugus</i>	Kurta, A. & Smith, S.M. 2014. Northeastern Naturalist 21(4):587-606	MI
<i>Myotis lucifugus</i>	Langwig, K.E., et al. 2012. Ecology Letters 15(9):1050-1057	NY
<i>Myotis lucifugus</i>	Layne, J.N. 1958. The American Midland Naturalist 60(1):219-254	IL
<i>Myotis lucifugus</i>	Martin, R.L., et al. 1966. Journal of Mammalogy 47(2):348-349	NY
<i>Myotis lucifugus</i>	McManus, J.J. 1974. Journal of Mammalogy 55(4):844-846	NJ
<i>Myotis lucifugus</i>	Pearson, E.W. 1962. Journal of Mammalogy 43(1):27-33	IL
<i>Myotis lucifugus</i>	Reimer, J.P. 2014. Northwestern Naturalist 95(3):277-289	AB
<i>Myotis lucifugus</i>	Royal Ontario Museum Life Sciences Division & Fenton, M.B. 1972†	ON
<i>Myotis lucifugus</i>	Storm, J.J. & Boyles, J.G. 2011. Acta Theriologica 56(2):123-127	NY
<i>Myotis lucifugus</i>	Vanderwolf, K.J. 2012. The Canadian Field-Naturalist 126(2):125-134	NB
<i>Myotis velifer</i>	Avila-Flores, R. & Mendellin, R.A. 2004. Journal of Mammalogy 85(4):675-687	MEX
<i>Myotis velifer</i>	Ayala-Boerdon, J. & Solis-Cardenas, V. 2017. THERYA 8(2):171-174	MEX
<i>Myotis velifer</i>	Caire, W. & Loucks, L.S. 2010. The Southwestern Naturalist 55(3):323-330	OK
<i>Myotis velifer</i>	Forbes, J. 1998. Journal of Cave and Karst Studies 60(1):27-32	NM
<i>Myotis velifer</i>	Hahn, W.L. 1908. Indiana University, 95:135-164	IN
<i>Myotis velifer</i>	Hayward, B.J. 1961. University of Arizona, Thesis	AZ
<i>Myotis velifer</i>	Jagnow, D.H. 1998. Journal of Cave and Karst Studies 60(1):33-38	NM
<i>Myotis velifer</i>	Reisen, W.K. et al. 1976. Journal of Parasitology 62(4):628-635	OK
<i>Myotis velifer</i>	Tinkle, D.W. and Patterson, I.G. 1965. Journal of Mammalogy 46(4):612-633	OK, KS
<i>Myotis velifer</i>	Twente, J.W. 1955. Ecology 36(4):706-732	TX
<i>Perimyotis subflavus</i>	Brack V. & Twente J.W. 1985. Canadian Journal of Zoology 63:2952-2954	MO
<i>Perimyotis subflavus</i>	Brack V. 2007. Environ Manage 40:739-746	OH

<i>Perimyotis subflavus</i>	Briggler J.T. & Prather J.W. 2002. American Midland Naturalist 149(2):406-412	AR
<i>Perimyotis subflavus</i>	Cox T.J. 1965. Journal of Mammalogy 46(4):687-688	MI
<i>Perimyotis subflavus</i>	Goehring, H.H. 1954. Journal of Mammalogy 35(3):434-436	MN
<i>Perimyotis subflavus</i>	Hahn, W.L. 1908. Indiana University, 95:135-164	IN
<i>Perimyotis subflavus</i>	Hall, J.S. 1962. Scientific Publications 12:3-68	KY
<i>Perimyotis subflavus</i>	Layne, J.M. 1958. American Midland Naturalist. 60(1):219-254	IL
<i>Perimyotis subflavus</i>	Pearson E.W. 1962. Journal of Mammalogy 43(1):27-33	IL
<i>Perimyotis subflavus</i>	Rice, D.W. 1957. Journal of Mammalogy 38(1):15-32	FL
<i>Perimyotis subflavus</i>	Rysgaard, G.N. 1942. The American Midland Naturalist 28(1):245-267	MN
<i>Perimyotis subflavus</i>	Sandel et al. 2001. Journal of Mammalogy 82(1):173-178	TX
<i>Perimyotis subflavus</i>	Swanson, G. & Evans C. 1936. Journal of Mammalogy 17(1):39-43	MN

Winter duration. The duration of winter hibernation is a critical component to understanding the metabolic demands of many bat species as insect resources typically disappear from the landscape during the coldest portions of the year. Despite this, relatively little information is available for the duration of this period and to-date no continuous estimation exists for North American bats. Therefore we estimated the winter hibernation period based on *Myotis lucifugus* as it is one of the most abundant and best studied bats in North America with a distribution spanning across the majority of the temperate zone (below the Arctic Circle and above the Tropic of Cancer). Records on bats immingence and emergence from hibernacula or duration of hibernation were collected from the literature, acoustic surveys, and from personal communications with local bat research groups (Hranac et al. accepted). The duration of hibernation was extracted from each location and a generalized linear model was used to correlate the number of days bats spend in winter hibernation and several abiotic variables. The top model selected by Akaike information criterion included terms for latitude, elevation, and the number of days of frost per year. Results were then projected back across the study extent to create a continuous estimation of the hibernation period (i.e., duration of winter) across the entirety of temperate North America (Hranac et al. accepted). All relevant code and products can be obtained from <http://github.com/cReedHranac/wintor>.

Literature Cited

- Haase, C.G., Fuller, N.W., Hranac, C.R., Hayman, D.T.S., McGuire, L.P., Norquay, K.J.O., Silas, K.A., Willis, C.K.R., Plowright, R.K., Olson, S.H. 2019. Incorporating evaporative water loss into bioenergetic models of hibernation to test for relative influence of host and pathogen traits on white-nose syndrome. PLoS One 14(10), e0222311.
- Hayman, D.T., Pulliam, J.R., Marshall, J.C., Cryan, P.M. and Webb, C.T. 2016. Environment, host, and fungal traits predict continental-scale white-nose syndrome in bats. Science Advances 2(1):e1500831.
- Hranac, C., Haase, C., Fuller, N., McClure, M. Marshall, J., Lausen, C., McGuire, L., Olson, S., Hayman, D. Accepted. What is winter? Modelling spatial variation in bat host traits and hibernation and their implications for overwintering energetics. Ecology & Evolution. Preprint available via Authorea (DOI: 10.22541/au.161185857.74191912/v1)
- McClure, M.L., Crowley, D., Haase, C.G., McGuire, L.P., Fuller, N.W., Hayman, D.T., Lausen, C.L., Plowright, R.K., Dickson, B.G. and Olson, S.H., 2020. Linking surface and subterranean climate: implications for the study of hibernating bats and other cave dwellers. Ecosphere 11(10):e03274.
- Perry, R.W. 2013. A review of factors affecting cave climates for hibernating bats in temperate North America. Environmental Reviews 21(1):28-39.

Appendix 2: Additional figures

	CRCM5 (UQAM)	CRCM5 (OURANOS)	RCA4	RegCM4	WRF	CanRCM4	HIRHAM5		
ERA-Int	0.44° 0.22° 0.11°	0.22°	0.44°	50km 25km	50km 25km	0.44° 0.22°	0.44°	RCP	ECS (°C)
HadGEM2-ES				50km 25km	50km* 25km*			4.5	4.6
								8.5	
CanESM2	0.44°		0.44°			0.44° 0.22°		4.5	3.7
	0.44° 0.22°	0.22°	0.44°			0.44° 0.22°		8.5	
MPI-ESM-LR	0.44°							4.5	3.6
	0.22° 0.44°	0.22°		50km* 25km*	50km 25km			8.5	
MPI-ESM-MR	0.44°							4.5	3.4
	0.22°							8.5	
EC-EARTH†			0.44°					2.6	~3.3
			0.44°				0.44°	4.5	
			0.44°				0.44°	8.5	
GFDL-ESM2M		0.22°		50km 25km	50km* 25km*			4.5	2.4
								8.5	
Access	PoC	PoC	ESGF	PoC	PoC	CCCma	ESGF		
Institution	UQAM	OURANOS	SMHI	Iowa State *NCAR	U Arizona *NCAR	CCCma	DMI		
Modeler	K. Winger	S. Biner	G. Nikulin	R. Arritt *M. Bukovsky	H-I Chang *M. Bukovsky	J. Scinocca	O. Christensen		

Figure A1. Matrix overview of projected climate data available via NA-CORDEX (adapted from <https://na-cordex.org/simulation-matrix.html>) and projections selected for this analysis (blue). Regional climate models (RCMs) are arranged as columns, and the global circulation models (GCMs) used to define the boundary conditions for each RCM run are arranged as rows. The columns at right define the representative concentration pathway (RCP), i.e., the greenhouse gas emissions scenario assumed for each model run, as well as the equilibrium climate sensitivity (ECS), a metric of relative severity of projected change suggested by each model.

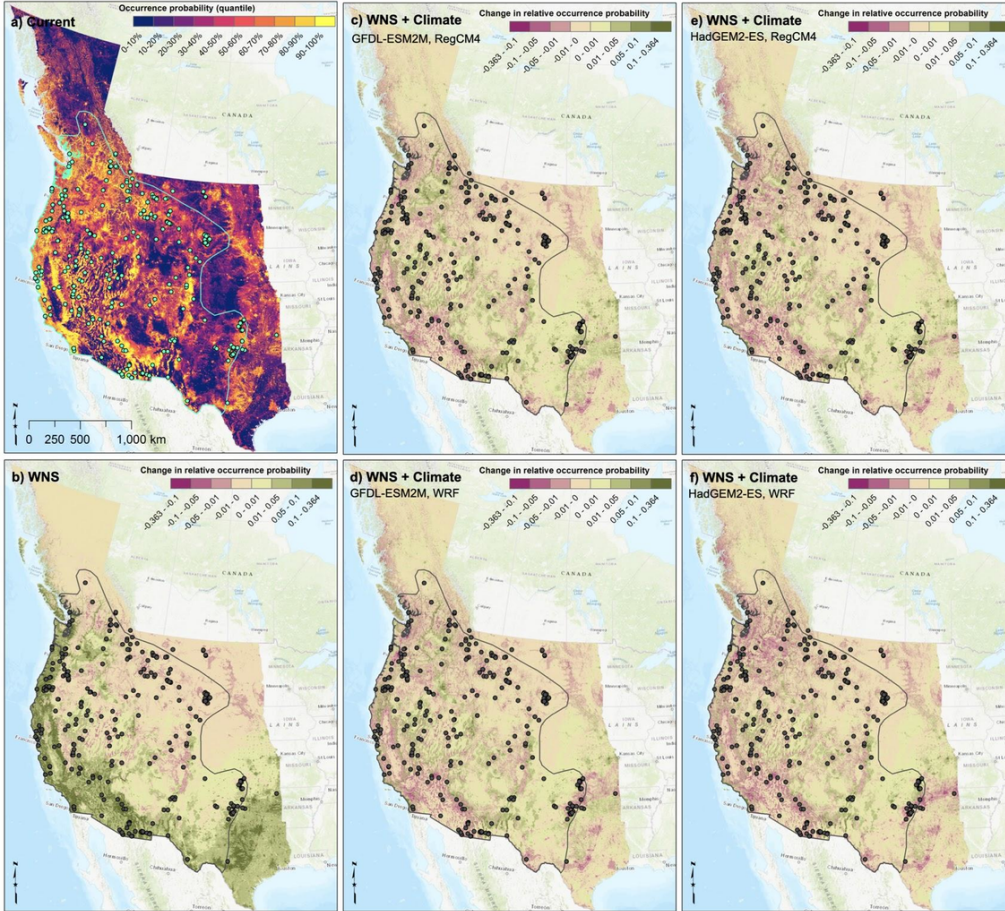


Figure A2. Projected change in *Corynorhinus townsendii* relative probability of occurrence (a) under multiple future scenarios: exposure to white-nose syndrome (WNS) under current climate conditions (b) and exposure to WNS under projected mid-century climate conditions (c-f). Future climate scenarios were driven by each combination of two global circulation models (GCMs): GFDL-ESM2M (c-d) and HadGEM2-ES (e-f) and two dynamically-downscaled regional climate models (RCMs): RegCM4 (c,e) and WRF (d,f). Darker green indicates a projected increase in occurrence probability; darker purple indicates a projected decrease. The species' current known range (gray outline) and points of recorded winter occurrence (gray points) are overlaid.

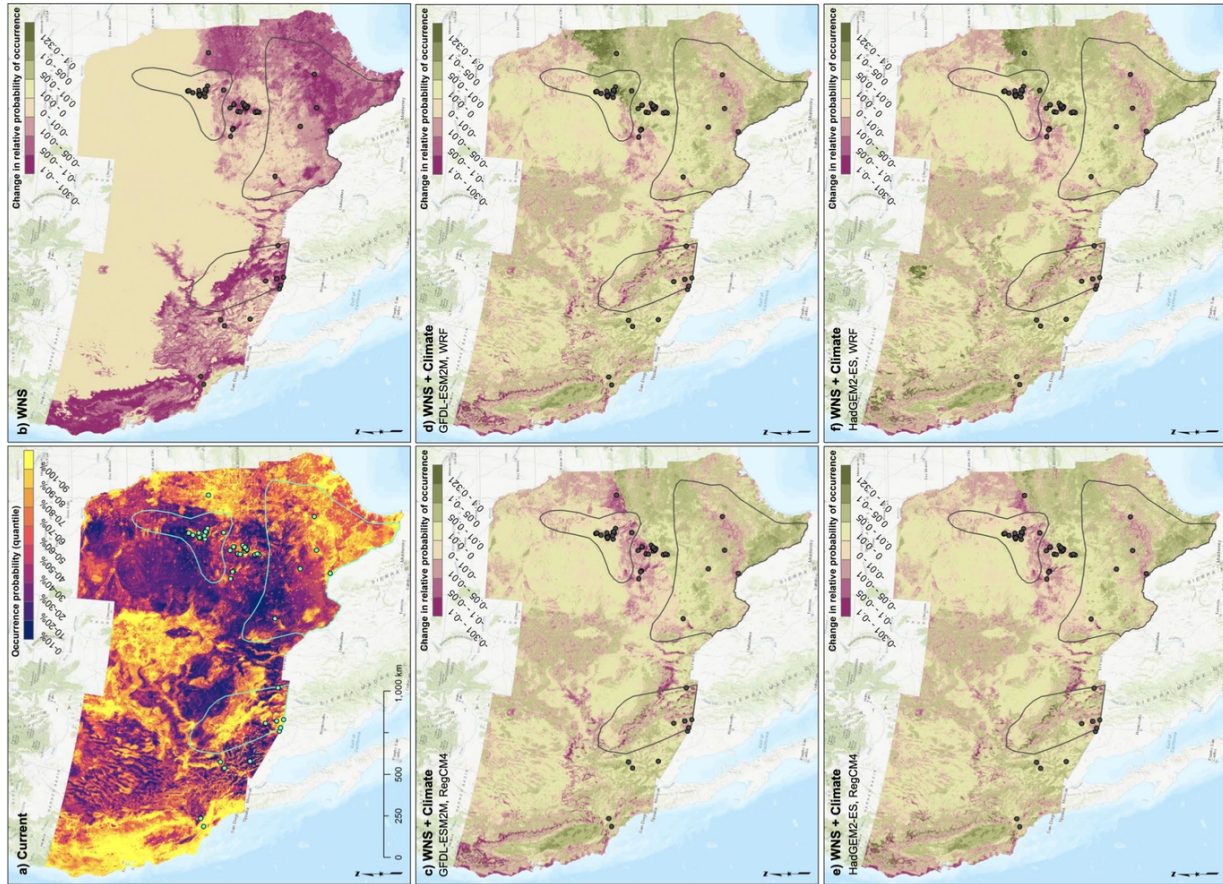


Figure A3. Projected change in *Myotis velifer* relative probability of occurrence (a) under multiple future scenarios: exposure to white-nose syndrome (WNS) under current climate conditions (b) and exposure to WNS under projected mid-century climate conditions (c-f). Future climate scenarios were driven by each combination of two global circulation models (GCMs): GFDL-ESM2M (c-d) and HadGEM2-ES (e-f) and two dynamically-downscaled regional climate models (RCMs): RegCM4 (c,e) and WRF (d,f). Darker green indicates a projected increase in occurrence probability; darker purple indicates a projected decrease. The species' current known range (gray outline) and points of recorded winter occurrence (gray points) are overlaid.